Faraday Discussions

Accepted Manuscript

This manuscript will be presented and discussed at a forthcoming Faraday Discussion meeting. All delegates can contribute to the discussion which will be included in the final volume.

Register now to attend! Full details of all upcoming meetings: http://rsc.li/fd-upcoming-meetings

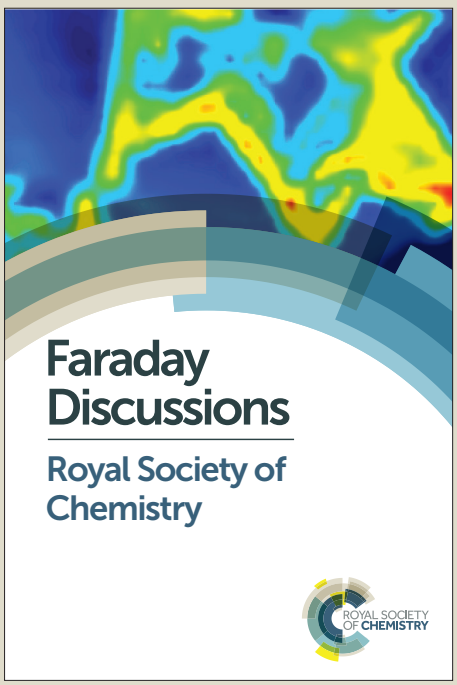

This is an *Accepted Manuscript*, which has been through the Royal Society of Chemistry peer review process and has been accepted for publication.

Accepted Manuscripts are published online shortly after acceptance, before technical editing, formatting and proof reading. Using this free service, authors can make their results available to the community, in citable form, before we publish the edited article. We will replace this *Accepted Manuscript* with the edited and formatted *Advance Article* as soon as it is available.

You can find more information about *Accepted Manuscripts* in the Information for Authors.

Please note that technical editing may introduce minor changes to the text and/or graphics, which may alter content. The journal's standard Terms & Conditions and the Ethical guidelines still apply. In no event shall the Royal Society of Chemistry be held responsible for any errors or omissions in this *Accepted Manuscript* or any consequences arising from the use of any information it contains.

ROYAL SOCIETY OF CHEMISTRY

www.rsc.org/faraday_d

Organic semiconducting single crystals as solid-state sensors for ionizing radiation

Beatrice Fraboni,* Andrea Ciavatti, Laura Basirico' and Alessandro Fraleoni-Morgera

DOI: 10.1039/b000000x [DO NOT ALTER/DELETE THIS TEXT]

Organic semiconductors have been so far mainly proposed as detectors for ionizing radiation in the indirect conversion approach, i.e. as scintillators, which convert ionizing radiation into visible photons, or as photodiodes, which detect visible photons coming from a scintillator and convert them into an electrical signal. The direct conversion of ionizing radiation into an electrical signal within the same device is a more effective process than the indirect one, since it improves the signal-to-noise ratio and it reduces the device response time. We report here the use of Organic Semiconducting Single Crystals (OSSCs) as intrinsic direct ionizing radiation detectors, thanks to their stability, good transport properties and large interaction volume. Ionizing radiation X-ray detectors, based on low-cost solution-grown OSSCs are here shown to operate at room temperature, providing a stable linear response with increasing dose rate in atmosphere and in radiation-hard environments.

1 Introduction

The detection of ionization radiation (e.g. X-rays, electrons and alpha particles) is a constantly growing area of research thanks to its vast and numerous application fields, that span from astrophysics to nuclear power plants, to industrial and civil security and to medical imaging and diagnostics.

High energy photons (X- and gamma-rays) can be detected with two different categories of functional materials: scintillators and semiconductors. In both cases, the interaction with an high energy photon induces at first primary excitations and ionization processes (ions and electrons) that, at a second stage, interact within the volume of the detection material and produce a majority of secondary excitations (electron-hole pairs), within a picosecond timeframe. The by-products of both primary and secondary excitations are electron-hole pairs (excitons) that can be transduced into an output signal following different pathways in semiconductor detectors and in scintillators, as better detailed in the following [1].

In a scintillator, the excitons transfer their energy to luminescent centers that are often intentionally introduced. These centers release the energy radiatively, and the resulting photons, typically in the visible wavelength range, escape the scintillator and are collected by a coupled photo-multiplier tube (PMT) or a photodiode to obtain an electrical signal associated to the incident radiation beam.

In a semiconductor detector (e.g. CdTe, SiC), an electric field is applied to dissociate the electron-hole pairs and to sweep the electrons and holes to the positive and negative electrodes, respectively. The resulting photocurrent is directly recorded

as the output electrical signal associated to the high energy radiation particles. The direct conversion of ionizing radiation into an electrical signal within the same material, and thus within one single device, is a more effective process than the indirect one, since it improves the signal-to-noise ratio and it reduces the device response time.

The material requirements for the two different detection mechanisms share some similarities: high stopping power to maximize the absorption efficiency of the incident radiation, high purity to minimize exciton trapping, good uniformity to reduce scattering and good transparency, possibly coupled to the ability to grow material into large size to increase the interaction volume. For semiconductors, a high and balanced carrier mobility and a low intrinsic carrier density are essential to obtain a high sensitivity and a low background current. On the other hand, scintillators must have an efficient cascade energy transition series to achieve a high light emission yield [2].

Among the novel materials that could push the boundaries of radiation detection further, organic π-conjugated small molecules and polymers are emerging interesting candidates, thanks to their potential to realize large area and flexible optoelectronic devices [3] by cost effective printing methods [4], due to their processing from solution at room temperature. Moreover, by controlling the molecular structure and the π-electron conjugated chains, their luminescent and optoelectronic properties can be easily tuned. In fact, it is known that organic semiconductors can work as effective photodetectors, via photoinduced generation of excitons that, within the material and in suitable conditions (presence of a local electron donor-electron acceptor interface usually formed at the interface between two different organic semiconducting materials) are able to split into free charge carriers that can be collected at the electrodes [8].

For this reason, organic semiconductors are now seen as an attractive alternative to inorganic compounds for photon detection in the region from UV to the near Infrared (NIR) where, besides the vast field of organic photovoltaic devices [5], also light pulse detectors for optical communications [6] and digital flat-panel arrays for imaging applications [7] have been proposed in the literature [8].

In the UV-NIR range, very interesting values for figures of merit such as photo-conversion efficiency, speed and minimum detectable signal level have been reported [8], and even though the simultaneous attainment of all these relevant parameters is demonstrated only in a limited number of papers, real applications are within reach for this technology, where the best reported photo-responsivities outperform amorphous silicon-based devices. Such achievements have been obtained by overcoming a few major bottlenecks for organic electronic devices, such as current injection from contacts to reduce leakage currents, charge collection efficiency and the stability to air exposure [8].

Organic materials could be viable candidates also for the detection of higher energy photons (X- and gamma-rays), and they were first suggested for radiation detection in the early 1980s [9]. However, the interest in these materials was mostly focussed on their scintillating properties [1], possibly because the material requirements are particularly stringent in the case of direct detectors, as evidenced by the few reports present in the literature on radiation detection based on organic thin films [10-14], where stability, reproducibility and the attainment of a good sensitivity (likely limited by the small interaction volume) are still open issues.

In this report we will discuss the very interesting ad promising radiation detecting

properties of a particular class of semiconducting organic materials: Organic Semiconducting Single Crystals (OSSCs).

We have recently reported how solution-grown OSSCs are ideal candidates to directly detect X-ray radiation (i.e. to directly convert an X-ray photon into an electron), thanks to their particular properties, that will be discussed in detail in the following paragraph, coupled to all the above mentioned advantages offered by organic conjugated materials [15]. Moreover, being based on Carbon, their low effective atomic number is similar to the average human tissue-equivalent Z and makes them ideal candidates for radiotherapy and medical applications that would benefit greatly from the improved accuracy of tissue-equivalent dosimeters. In fact, there are currently no low-cost, large-area detectors with tissue-equivalence response available.

It is noteworthy that, unlike organic photodiodes, OSSCs showed direct and intrinsic charge photogeneration and collection processes with no need for the heterogeneous donor-acceptor material interface, usually employed to improve the collection efficiency in organic photodiodes and solar cells.

We will assess here the reproducible process of conversion of X-ray photons into an electrical signal within OSSCs, and how this process allows to fabricate stable radiation detectors that provide a linear response to an increasing X-ray dose. The observed performance indicates that OSSCs are very promising candidates for a novel generation of low-cost, real-time and room-temperature operated X-ray detectors.

2 Semiconductor-based direct detectors

The ability to detect high energy radiation such as X-rays, gamma-rays, and other uncharged and charged particles with solid-state semiconductor detectors has improved dramatically in the last 20 years thanks to two main factors: i) the enormous advances in the semiconductors science and technology and ii) the strong and increasing demand of highly performing solid-state radiation detectors.

High purity Silicon and Germanium were the first materials to be used as solid-state detectors, and still are widely employed thanks to their extremely good energy resolution (below 0.2%) that, however, can only be achieved at cryogenic temperatures. This prompted the development of novel compound semiconductors such as CdTe, SiC and CdZnTe that can offer excellent performance at room temperature, superior for a few aspects to Ge.

Nonetheless, the difficulty to grow large-size, high-quality crystals of these II-VI compound materials at low costs is limiting their applications to very high-tech and specific detectors, e.g. in satellites and as pioneering medical diagnostic tools. A non-negligible further drawback of these materials is their limited availability, and often their toxicity. These limitations prompt the need to find alternative novel semiconducting materials.

The main requirements for a good solid state semiconductor detector, are common to all semiconductors and are briefly detailed below [1,16]:

a) High resistivity (>10^9 Ωcm) and low leakage current. Low leakage currents when an electric field is applied during operation are critical for low noise operation. The necessary high resistivity is achieved by using larger bandgap

materials (>1.5 eV) with low intrinsic carrier concentrations

b) Small enough bandgap so that the electron-hole ionization energy is small (<5 eV). This ensures that the number of electron-hole pairs created is reasonably large and results in a higher signal to noise ratio.

c) High atomic number (Z) and/or a large interaction volume for efficient radiation-atomic interactions. The cross-section for photoelectric absorption in a material of atomic number Z varies as Z^n, where $4 < n < 5$. For high-sensitivity and efficiency, large detector volumes are required to ensure that as many incident photons as possible have the opportunity to interact in the detector volume. A further related requirement is that the detector material must have a high density, although this is essentially guaranteed simply by the fact that a solid material is employed for the detector material in contrast to gas-based detectors.

d) High intrinsic $\mu\tau$ product. The carrier drift length is given by $\mu\tau E$, where μ is the carrier mobility, τ the carrier lifetime, and E the applied electric field. Charge collection is determined by which fraction of photo-generated electrons and holes effectively traverses the detector and reaches the electrodes.

e) High-purity, homogeneous, defect-free materials, to ensure good charge transport properties, low leakage currents, and no conductive short circuits between the detector contacts.

f) Electrodes that produce no defects, impurities or barriers to the charge collection process and which can be used effectively to apply a uniform electric field across the device. This requirement is also related to the need to avoid material polarization effects that may affect the time response of the detector.

g) Surfaces should be highly resistive and stable over time to prevent increases in the surface leakage currents over the lifetime of the detector.

It is obvious that not all the above requirements can be easily met by a single material, but the dramatic advancements in the organic semiconductor research field recently stimulated studies on the potential application of organic semiconductors as solid-state detectors.

The first studies were performed on neutron irradiation of polyacetylene and polythiophene films that induced an increase in the film conductivity, linear with the irradiation dose but irreversible [17]. Up to date, only a few examples of simple, direct detectors based on organic semiconductors are reported, and they all refer to thin films based on organic semiconducting polymers [11,12,14] and small molecules [13].When compared to silicon-based detectors conjugated polymers, despite their lower carrier mobility and inferior radiation tolerance, exhibit the advantage that large areas can be covered and possibly nanostructured via wet-processing, thus increasing the detector active surface at a much lower cost [18].

The already mentioned issue of degradation of semiconducting polymers represents a practical problem for the fabrication of effective semiconducting polymer-based intrinsic, direct detectors. In fact, many of the above cited detectors base their operability on the measurement of the resistivity (conductivity) of the polymeric semiconductor, which increases (decreases) upon device exposure to the ionizing radiation, due to material degradation. This means that the above described devices are not able to perform for prolonged times, neither to be repeatedly used with reproducible performances, resulting hence as detectors with a very short operative lifetime and, in the best possible case, as disposable devices.

A first step towards the solution of these problems was made recently, when

semiconducting polymers-based drop-cast films with a thickness of approximately 10-20 μm (hence a rather thick film, to maximize X-ray attenuation) showed linearity up to dose rates of 60 mGy/s [13,14]. The sensitivity of these devices reached values of 100-400 nC/mGy/cm^3, which are comparable to silicon devices. The time response of the X-ray photocurrent measured for the thin film devices was less than 150 ms, and encouragingly, no sign of radiation damage was observed for doses in excess of 10 Gy, although no particular accent on reproducibility of the results was reported [13,14].

Though the authors of these reports do not always mention it explicitly, it has to be noticed that in these devices the polymeric semiconductors thin films are always coupled to metallic electrodes or substrates, which are exposed to the ionizing radiation together with the organic layer. The importance and the role of the metallic electrodes and/or the substrate in the performance of these devices are stressed out in several dedicated works, [6,7,13], since they act as the primary X-ray photo-conversion layers, producing the secondary electrons that are injected into the organic thin film and thus produce the electrical signal output.

We have recently reported how solution-grown OSSCs are ideal candidates to directly detect X-ray radiation as their particular properties allow to overcome most of the major limitations inherent to organic materials discussed up to now [15]. Their long-range molecular packing order and lack of grain boundaries impart all OSSCs unique transport properties such as top carrier mobilities (up to 40 cm^2/Vs [19]), transport anisotropy and long exciton diffusion length (up to 8 μm [20] as opposed to the few nanometers in organic thin films and blends used in photovoltaic and photodetecting devices [8]). These features, coupled to their high resistivity, and low dark currents due to the relatively large band gap, are enhanced, in the case of solution-grown OSSCs, by the possibility to tune the crystals dimensions up to mm^3, as will be discussed in more detail in the next paragraph. Moreover, a notable unique property of OSSCs is that they can efficiently and intrinsically photo-convert the X-ray photons into electrical signal, without the need of extra metal/substrate layers intervention [15].

3 Solution-grown Organic Semiconducting Single Crystals

Top performing OSSCs are usually grown using chemical vapour deposition (CVD), which involves the use of multi-zone heated tubes, in which a vapour of molecules is carried by a convenient inert gas onto a cold wall, but due to the nature of this growth process, it is difficult to grow very large crystals[21]. Crystal growth from the melt could represent an interesting alternative to CVD, nonetheless, although in some cases crystallization from the melt of OSSCs proved to be successful [22], stability problems (especially due to enhanced photo-oxydation rates at temperatures approaching the melting ones) often limit the possibility of taking advantage of this crystallization technique for organic materials.

These problems may be overcome using growth from solution. This approach has a high versatility, with the capability to deliver very large (up to several cm^3) and pure crystals, low energy requirements (i.e. no need for dramatic heating, cooling or vacuum) and easiness of implementation. This latter point is worth of particular attention, since it implies extremely low costs, especially when large-area detectors are envisaged.

Solution growth has also been used to produce organic (not necessarily semiconducting) single crystals used as scintillators in ionizing radiations detectors [23], evidencing that this technique delivers crystals able to usefully interact with ionizing radiations. In addition, solution-grown OSSCs have repeatedly demonstrated good electronic quality [24]. The possibility of growing OSSCs from solution offers not only exciting chances of performing fundamental studies, but, even more interestingly, paves the way for promising practical application of these materials in electronic devices. In fact, it has been recently shown that it is possible to fabricate high-quality OSSCs via inkjet printing [25] or shear-aided crystallization [26].

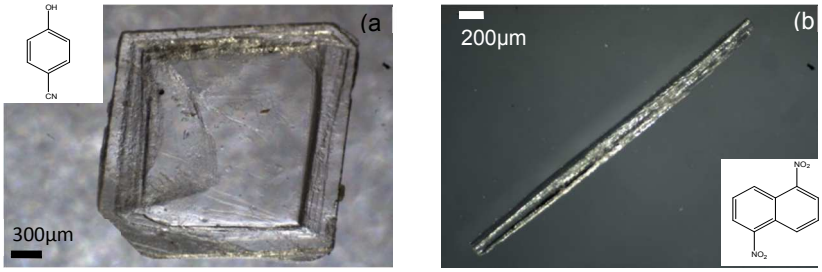

Figure 1: Optical microscopy images of (a) 4-hydroxycyanobenzene (4HCB) and (b) 1,5-dinitronaphthalene (DNN) organic single crystals. The images clearly shows the different shapes of the crystal, i.e. the platelet shape of 4HCB and the needle-like shape of the DNN crystal. In the inset the chemical structures of the two molecules are also reported.

We will report here on two different types of OSSCs that we have grown from solution: 4-hydroxycyanobenzene (4HCB) and 1,5-dinitronaphthalene (DNN), shown in Figure1.

These two molecules have been chosen because they generate crystals with different geometry: platelets in the case of 4HCB and needles for DNN. Both types of crystals can be easily grown from widely available solvents/non solvents (i.e. ethylic ether and/or petroleum ether for 4HCB [27] and chloroform or benzonitrile for DNN), and their size can be controlled working on parameters like solvent/non solvent volume ratios or the organic molecule concentration in the starting solutions, reaching sizes up to tens of mm^3. This translates into a radiation interaction volume much larger than those typically accessible with polymer films (that area few tens of micrometers thick at most) [27]. The so-obtained single crystals are very robust to physical manipulation (they can be easily moved and positioned on substrates, electrodes arrays, sample holders, etc.) and to environmental conditions (air, light, room temperature).

It is known that the low symmetry of organic molecules leads to anisotropically packed crystal structures, where the direction of the strongest π-orbitals overlap usually coincides with the direction of the highest carrier mobility, thus also affecting the crystal transport properties [19,21,28]. On one hand this asymmetry introduces difficulties for clearly understanding the transport behaviour of the organic crystal, but on the other hand it offers the possibility to investigate the correlation between the three-dimensional molecular stacking order of OSSCs and their known anisotropic electronic transport properties. In particular, in the last years different mobilities have been measured along the three dimensions for micro or nanometer sized organic single crystals, either vapour deposited [19,21,28] or solution-grown [24,29-31].

A complete characterization of several key electronic transport parameters of OSSCs can be carried out by means of Space Charge Limited Current (SCLC) [21,29,31,32] and by Field Effect Transistor (FET) analyses [29,30].

We have recently reported on the electrical characterization of solution-grown, macroscopic 4HCB single crystals, evidencing their good electronic transport properties and their clear anisotropic behaviour along the three crystallographic axes [29,31], and we will here focus our attention on the results obtained for DNN single crystals. Due to their needle-like shape, there is basically only one crystallographic direction that can be electrically accessed and that coincides with the higher π-orbitals overlap direction (as visible examining the DNN crystal structure [33]). The good electronic transport properties of DNN single crystals have been assessed by SCLC analyses and a typical SCLC curve of a DNN crystal is shown in Figure 2 together with a sketch of the electrical contacts configuration. The intrinsic carrier mobility of the material is reported in Table 1 together with the average carrier mobility determined for 4HCB crystals, also from SCLC analyses, along the three crystallographic directions.

Crystal	μ_{SCLC} (cm^2/Vs)
4HCB	
a axis	$(1.0 \pm 0.5) \times 10^{-1}$
b axis	$(4 \pm 2) \times 10^{-2}$
c axis	$(2.0 \pm 0.5) \times 10^{-5}$
DNN	$(2.2 \pm 0.8) \times 10^{-3}$

***Table I**: Carrier mobility values reported in literature [29-31] for a 4HCB crystal along the three crystallographic axes a,b and c in comparison with the mobility value measured for a DNN crystal along its axis of growth (only one since it's needle-shaped).*

Indeed, as shown in Table I, the transport properties of 4HCB crystals reflect its anisotropic packing, and a clear difference in mobility values is found along the three axes. Charge carrier mobilities of 0.1 cm^2/Vs can be easily and routinely obtained along the a axis of 4HCB solution-grown crystals, with very reproducible and stable results [31]. While the anisotropic electrical response of OSSCs is extremely interesting from the point of view of fundamental studies, it poses the problem of properly aligning the crystals and the electrodes in order to select and control the appropriate carrier transport properties needed for specific device applications. Even if we have demonstrated how linearly polarized infrared analyses allow a fast, easy and reliable determination of the crystallographic orientation of OSSCs [34,35], it is important to investigate the X-ray photoresponse of single crystals where the electronic transport axis is clearly identifiable. For this reason needle-like crystals, such as DNN, could be of practical interest.

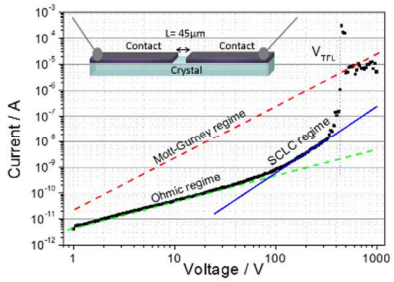

***Figure 2:** Current vs voltage curve, in double-logarithmic scale, of a DNN crystal with in evidence the space-charge conduction regime. The schematic layout of the electrical ohmic contacts on a DNN crystal is in the inset).*

4 X-ray photo-response of OSSCs

After having assessed that solution-grown 4HCB and DNN OSSCs have appropriate volume sizes and electronic transport properties to grant the collection of photo-generated charge carriers, we performed a complete characterization of the organic crystals electrical photoresponse under a Molybdenum (Mo) tube X-ray broad spectrum with accelerating voltage of 35kV and dose rate 2.5-140 mGy/s, All the reported measurements are made in air at room temperature.

Figure 3 reports for the first time typical Current-Voltage and Current-Time curves measured for a DNN crystal exposed to an X-ray beam from a Mo tube (35 keV, 140 mG/s), with two Ag electrodes evaporated at a distance of 45 μm, in the same configuration reported in the inset of Figure 2. The strong modification induced in the current measured as a function of applied voltage when the DNN crystal is exposed to X-rays beam, due to the photo-induced generation of charge carriers, is visible in Figure 3a. It is noteworthy that this sharp response was obtained with applied voltages as low as 2 V, a very small value for radiation detectors. Moreover, the "off" current recorded after the exposure to X-rays does not show significant hysteresis or degradation effects and its value lies always below 500 pA, again a very good low value for radiation detection applications. A further positive feature of this device is that the current vs. time curve recorded under an on/off switching X-ray beam (Figure 3b) clearly shows how repetitive exposures to X-rays do not alter the sensor photo-response in terms of $\Delta I = I_{on} - I_{off}$ and baseline current shift. Figure 3c shows the virtually null effect of UV-Vis irradiation on the same crystal. It is hence evident that the physical processes generating the X-ray induced photo-response do not have much in common with those responsible for the UV-IR detection in organic photodiodes or phototransistors [8]

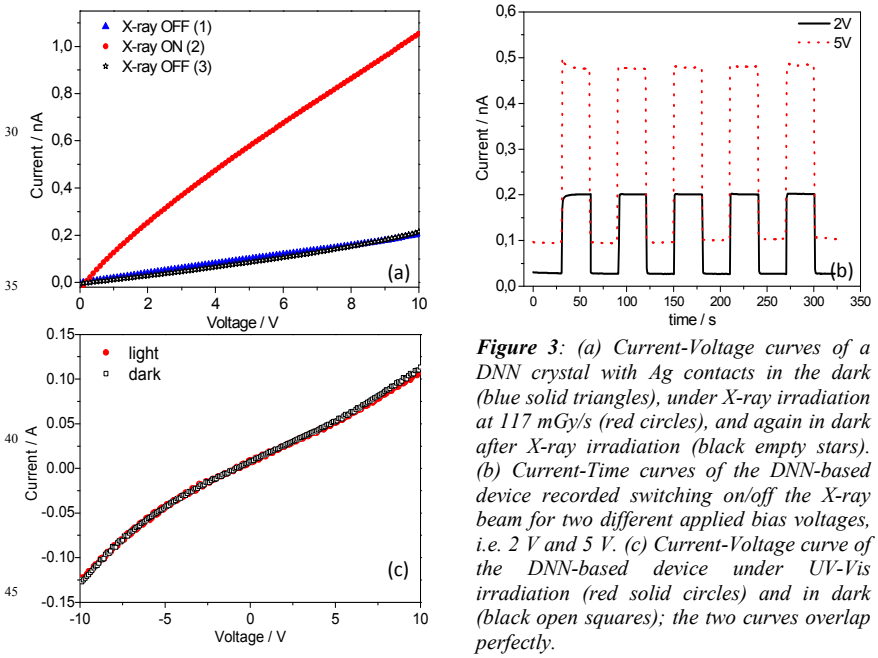

***Figure 3**: (a) Current-Voltage curves of a DNN crystal with Ag contacts in the dark (blue solid triangles), under X-ray irradiation at 117 mGy/s (red circles), and again in dark after X-ray irradiation (black empty stars). (b) Current-Time curves of the DNN-based device recorded switching on/off the X-ray beam for two different applied bias voltages, i.e. 2 V and 5 V. (c) Current-Voltage curve of the DNN-based device under UV-Vis irradiation (red solid circles) and in dark (black open squares); the two curves overlap perfectly.*

Several DNN crystals were tested under X-ray dose rates ranging from 20 to 120

mGy/s, at different bias voltages. The induced photocurrent values $\Delta I = I_{on}-I_{off}$, are reported in Figures 4a and 4b and demonstrate that the crystal response for an increasing X-ray dose rate is linear for each tested bias voltage, assessing that it is possible to effectively drive a OSSCs detector even at a few bias volts. The detector sensitivity, defined as $S = \Delta I / D$, where D is the radiation dose rate, was evaluated to be about 6 nC/mGy at 10 V.

Similar results had been obtained for 4HCB crystals in platelet shape, that showed a linear response to X-ray irradiation for bias values up to 500 V with X-ray photoinduced current variations ($\Delta I = I_{on}-I_{off}$) of up to ten nA [15]. The radiation hardness of OSSCs, i.e. their tolerance to high doses of ionizing radiation, is quite surprisingly high. Figure 5 shows the current vs. time curve of a 4HCB crystal, with an on/off switching 35 keV X-ray beam, before and after having received a total X-ray dose of about 2 kGy. The detector performance of the same 4HCB crystal has been measured again after 1 month of storage in the dark and its photo-response, again for a on/off switching 35 keV X-ray beam, is notably not altered. It is noteworthy that the $\Delta I = I_{on}-I_{off}$ value is quite stable both after strong irradiation and after prolonged aging, even if the baseline current obviously shifts a little, likely due to bulk radiation damage and/or degradation effects that could be located either within the crystal or at the electrodes.

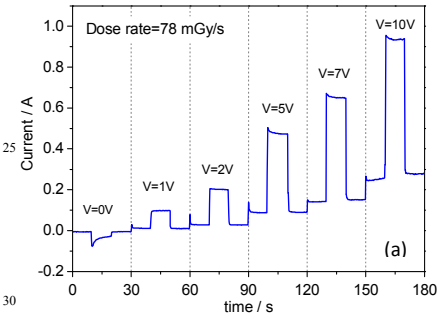

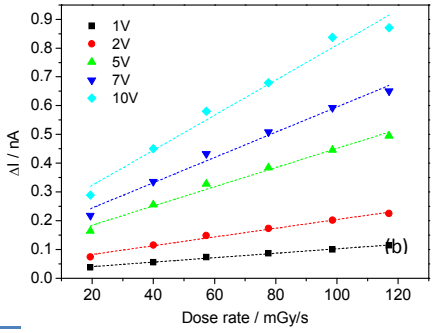

Bias (V)	Sensitivity (nC/Gy)
1	0.8
2	1.5
5	3.4
7	4.4
10	6.1

(c)

Figure 4: *(a) Current-Time curve of the DNN-based device recorded switching on/off the X-ray beam (dose rate of 78 mGy/s) and sweeping the bias voltage after each cycle. (b) X-ray induced current variation $\Delta I = I_{on}-I_{off}$ for increasing dose rates at different bias voltages. (c) Detector sensitivity values for different bias voltages, calculated from linear fit of the plots reported in (b).*

To investigate the role and effects of the molecular anisotropic packing in the X-ray photo-response of OSSCs it is useful to compare the responses of the DNN molecule that crystallizes in a needle-like shape and of the platelet shaped crystals obtained with 4HCB (Figure 1). While DNN crystals allow only to sample one crystal axis, the one parallel to the strongest π-stacking and faster crystal growth rate, 4HCB crystals allow to investigate their photo-response along all three crystallographic directions (inset of Figure 5). As can be inferred from the measured mobility values, the tighter π-stacking axes are the two planar ones (labelled a and b) which possess a good mobility, while the vertical axis c is characterized by a poorer π-stacking

degree and by a much smaller mobility (Table I) [29-31].

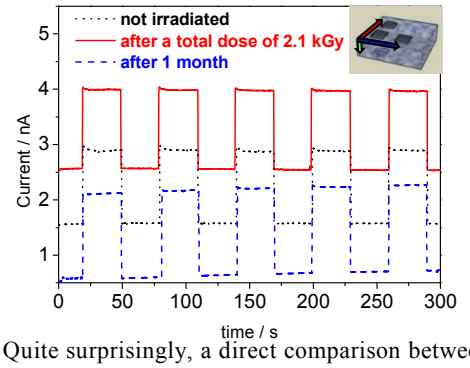

Figure 5: *Current-time curves recorded along axis c (see inset) under an on/off switching X-ray beam (35keV @ 150mGy/s) before (black dotted line) and after (red solid line) a total dose of 2.1 kGy; the blue dashed line indicates the same measure repeated after one month.*

Quite surprisingly, a direct comparison between the X-ray induced photocurrent of a 4HCB crystal in the vertical collection geometry (small electrode on the top and on the bottom of the crystal) and in the planar collection one (two small electrodes on the top crystal surface), in identical experimental conditions (i.e. the same electrode distance of of 200 μm and same X-ray irradiation conditions)shows that the X-ray sensitivity is smaller along the planar axes (7 vs. 24 nC/Gy at 10 V) despite the fact that the charge carrier mobility is about 3 order of magnitude higher than along the vertical axis (Figure 6). Moreover, the sensitivity is comparable along the main π-stacking axis for both DNN and 4HCB crystals (approx. 7 nC/Gy @10 V), that is accessed in both types of crystal with a planar electrode geometry.

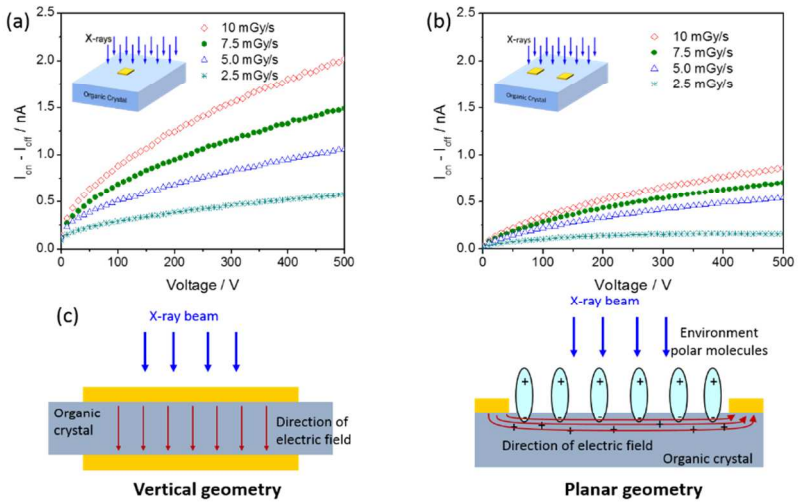

(d)

Bias (V)	Sensitivity (nC/Gy)		
	@10V	@50V	@100V
Planar	7	18	28
Vertical	24	49	70

Figure 6*: X-ray induced current variation of a 4HCB crystal in the vertical geometry (a) and in a planar geometry (b) for different X-ray doses. (c) Sketch of the electric field distribution in vertical and planar geometry. The hypothetical effect of polar environmental molecules at the crystal surface in the planar geometry is also shown. (d) Sensitivity values recorded for a 4HCB-based detector in planar and vertical geometry for three different bias voltages, i. e. 10 V, 50 V and 100 V.*

These results (i.e., the crystal axes characterized by the strongest π-stacking, that generally coincide with the best current transport axes, show a poorer X-ray photo-response) suggests that the planar electrode configuration is less performing independently from the crystals shape (either needle-like or platelet). Three main causes can be hypothesised for this behaviour:

i) the better electrical transport properties along crystal axes strong π-stacking may be a limiting factor with respect to the crystals sensitivity to X-rays, due to the higher off currents.

ii) the electric field distribution in the vertical geometry is much more effective in collecting the photogenerated carriers that in the planar one (see Figure 6c). In the vertical geometry the whole electrode area can actively collect the induced charge carriers, while only a thin region around the electrode edge is effective in the planar one, even if the exciton diffusion length in OSSCs has been recently assessed to be about 8 μm [20].

iii) the high polarizability of the π-electrons at the crystal surface, possibly further enhanced by the direct exposure to X-rays that are known to cause ionization of organic molecules, may result in interactions with polar environment molecules (water etc.), that when adsorbed at the surface can affect the carrier density distribution or trapping states in the first monolayer below the surface as sketched in figure 6c (an effect that is analogous to the operating principle of organic field effect transistors).

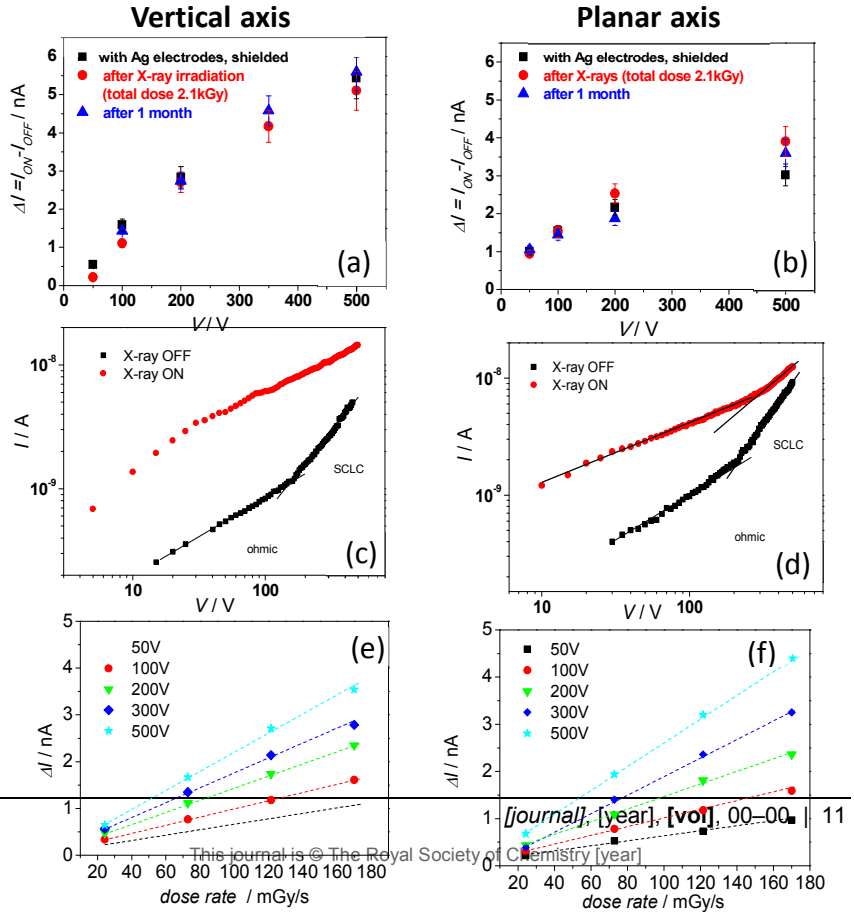

Figure 7: *Different X-ray induced photocurrent response of a 4HCB-based detector as a function of the bias voltage, collected along the vertical (a) and the planar (b) crystal axis, before (black squares) and after (red circles) a total dose of 2.1 kGy of X-ray irradiation and after one month (blue triangles). (c,d) Current-Voltage curves for the two axes in dark (black squares) and under X-ray irradiation (dose rate of 170 mGy/s). The lack of the ohmic-SCLC transition under irradiation is shown. (e,f) X-ray induced current variation ΔI =Ion –Ioff for increasing dose rates at different bias voltages along the two axes.*

Figure 7 (a and b) gives a better insight on the different ΔI ($=I_{on}-I_{off}$) response along the vertical and planar axes. The ΔI remains clearly smaller along the planar axes even after strong irradiation or a month-long aging. These results suggest that either the crystal surface plays a minor role in this measurements or its interaction with environment and atmosphere induces always the same effects even after the strong rad-hardness and aging tests that could have significantly altered the surface chemistry, its charge state or its conductivity. The current-voltage curves measured on the two axes of the same crystal in the dark (i.e. when the X-ray beam is off) (Figures 7c and d) follow the SCLC behaviour typical of high resistivity semiconductors [32]. However, it is noteworthy that under X-ray exposure the electrical response of our crystals along the vertical direction remains purely ohmic, while along the planar axes it follows the same SCLC behaviour found in the dark, even at higher voltages. This suggests that the electrically active traps that control the SCLC transport in the dark along the vertical axis play no major role when the crystal is probed under X-rays. From a wider perspective, it is remarkable that the strong 3D anisotropy in carrier mobility does not affect the resulting X-ray photoresponse and sensitivity, and that OSSCs can be reliably used as detectors along all three crystallographic directions, irrespective of the mobility value in the dark, as is verified by the good linear response to increasing X-ray dose rates along both planar and vertical axes (Figure 7e and f). However, the device electrode geometry appears to play a major role in the performance of the radiations detector, the vertical sandwich geometry being much more performing than the planar one (as also clearly shown in Figure 8 that shows the X-ray sensitivity for the planar and vertical axes of a 4HCB crystal under a 35 keV X-ray beam). Further research is ongoing to better clarify this issue [36].

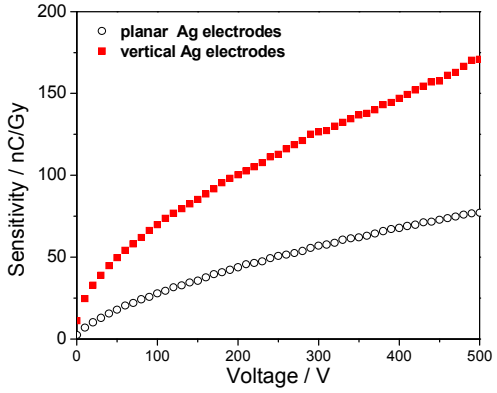

Figure 8: *Comparison between the sensitivity values at different bias voltages for a 4HCB-based detector under 35keV X-ray irradiation in planar (black circles) and vertical (red squares) electrodes configuration.*

5 Conclusions and outlook

Organic materials can be a novel and smart alternative to traditional inorganic semiconducting solid-state radiation detectors, due to their low cost, large availability and to the possibility of achieving novel functionalities like flexibility or transparency. In particular, OSSCs are better performing than organic thin films thanks to their following particular properties: a) low dark current thanks to the wide effective band gap; b) high degree of packing order; c) long exciton diffusion length; d) good carrier mobility; e) possibility to tune their volume up to mm^3; f) greater stability in air.

Solution-grown OSSCs based on different molecules can perform well as solid state radiation detectors, as we have shown for crystals based on the molecules 4HCB and DNN. The crystal shape and geometry does not affect the detector performance, since both needle-like (DNN) and platelet crystals (4HCB) have been successfully assessed as X-ray detecors. Even if the anisotropic packing of the molecule affects the electronic transport properties of the crystal, inducing carrier mobility that can vary up to 4 orders of magnitude along the three crystal axes, it is noteworthy that all axes can be used for an effective detection of ionizing radiation, paving the way to unprecedented radiation detector architectures. Interestingly, in 4HCB crystals the largest sensitivity is obtained in the vertical geometry, even if in this configuration the electrodes are not connecting the crystal axis with the best molecular π-stacking and carrier mobility. Further work is ongoing to better understand this point and the photo-physical processes generating the X-ray induced charge carriers, together with their transport and collection mechanisms within the organic semiconducting single crystal.

Acknowledgements

The authors acknowledge the financial support from the European Community under the FP7-ICT Project “i-FLEXIS” (GA n. 611070).

References

[a] *Dipartimento di Fisica e Astronomia, Università di Bologna , viale Berti Pichat 6/2, Bologna, Italy Fax: +39 051 2095113; Tel: +39 051 2095806; E-mail: beatrice.fraboni@unibo.it*
[b] *Dept. Of Engineering and Architecture, Univ. Of Trieste – V. Valerio 10, 34100 Trieste, Italy and Elettra Sincrotrone Triescte SCpA – SS 14, Km. 163.5, 34149 Basovizza (TS), Italy*

1 Glenn Knoll *“Radiation Detection and Measurement”,* Fourth Edition 2011 Wiley Ed.
2 Qi Chen, Tibor Hajagos and Qibing Pei, *Annu. Rep. Prog. Chem., Sect. C*, 2011, **107**, 298
3 H. Dong , H. Zhu , Q. Meng , X. Gong , W. Hu , *Chem. Soc. Rev.* 2012 , **41** , 1754 .
4 G. C. Schmidt , M. Bellmann , H. Kempa , M. Hambsch , K. Reuter , M. Stanel , A. C. Hübler , *MRS Online Proceedings Library* 2011, **1285** .
5 G.Dennler, M.C.Scharber, C.J.Brabec, *Adv.Mat.*2009, **21,** 1323; S.Gunes,H.Neugebauer, N.S.Sariciftci*, Chem. Reviews* 2007, **107,** 1324.

6 T. Agostinelli,M.Caironi,D.Natali,etal., *J.Appl.Phys*. 2008, **104,**114508.
7 T.N.Ng,W.S.Wong,M.L.Chabinyc,S.Sambandan,R.A.Street, *Appl.Phys.Lett*. 2008, **92** 213303; P.E. Keivanidis, N.C.Greenham, H.Sirringhaus,etal.,*Appl.Phys.Lett*. 2008, **92** 023304.
8 K-J. Baeg, M. Binda, D.Natali, M.Caironi,Y-Y.Noh , *Adv.Mat* 2013 **25,** 4267; X.Gong, MH Tong, YJ Xia, WZ Cai, JS Moon, Y Cao, G Yu, CL Shieh, B Nilsson, AJ Heeger *Science* 2009, **325**,1665
9 K. Yoshino, S. Hayashi and Y. Inuishi*, Jpn. J. Appl. Phys. Part 2-Lett*., 1982**, 21**, L569; K. Yoshino, S. Hayashi, G. Ishii and Y. Inuishi, *Solid State Commun*., 1983, **46**, 405.
10 S. Graham , R. Friend , S. Fung , S. Moratti , *Synth. Met.* 1987 , **84** ,903 .
11 P. Beckerle , H. Ströbele , *Nucl. Instrum. Methods Phys. Res., Sect. A* 2000 , **449** , 302 .
12 F Boroumand,M.Zhu,A Dalton,J.Keddie P.Sellin,J.Gutierrez, *Appl.Phys.Lett*. 2007, **91** , 33509 .
13 A. Intaniwet , J. Keddie , M. Shkunov , P. Sellin , *Org. Electron.* 2011 ,**12** , 1903; Intaniwet A, Mills C A, Shkunov M, Thiem H, Keddie J L and Sellin P J *J. Appl. Phys.* 2009, **106** 064513;
14 A Intaniwet, C Mills, M Shkunov, P J Sellin and J L Keddie, Nanotechnology, 2012 **23** 235502.
15 B.Fraboni, A. Ciavatti, F. Merlo, L. Pasquini, A.Cavallini, A. Quaranta, A. Bonfiglio, A.Fraleoni-Morgera *Adv.Mater.* 2012 **24**, 2289
16 T. E. Schlesinger and R. B. James "*Semiconductors for Room Temperature Nuclear Detector Applications*" 1995 Academic Press, San Diego,
17 M. A. Butler, D. S. Ginley and J. W. Bryson, J.Electroch.Soc., 1984, **131**, C327.
18 A.Fraleoni-Morgera, G. Palma, J.Plaisier, *RCS Adv.* 2013 **3**, 15664; .Ph. Leclère, M. Surina, P. Brocorensa, M. Cavallini, F. Biscarini, R. Lazzaroni *Mater. Sci. Eng. R*, 2013 **55**, 16
19 V. Podzorov , E. Menard , A. Borissov , V. Kiryukhin , J.A. Rogers , M.E. Gershenson , *Phys. Rev. Lett*. 2004 **93** , 086602
20 H. Najafov, B. Lee, Q. Zhou, L. C. Feldman and V. Podzorov *Nature Mat.* 2009 **10**, 938
21 N. Karl, *J. Cryst. Growth,* 1990 **99** 1009; B.de Boer et al., *phys.stat.sol. a* 2004 **201**, 1302
22 K. Sankaranarayanan, P. Ramasamy, *J. Cryst. Growth* 2006 **292** 445
23 N. P. Zaitseva et al., *LLNL-JRNL-414904*, 2009, 1; G. Hull et. al., *IEEE Trans. Nucl. Sci*., 2009, **56**, 899
24 S. C. B. Mannsfeld, A. Sharei, S. Liu, M. E. Roberts, I. McCulloch, M. Heeney, Z. Bao, *Adv. Mater.* 2008, **20**, 4044; S. K. Park, T. N. Jackson, J. E. Anthony, D. A. Mourey, *Appl. Phys. Lett.*, 2007, **91**, 063514; Q. Tang et al., *Adv. Mater.* 2008, **20**, 2947.
25 H. Minemawari, T. Yamada, H. Matsui, J. Tsutsumi, S. Haas, R. Chiba, R. Kumai, T. Hasegawa, *Nature,* 2011, **475,** 364
26 Y. Diao, B. C-K. Tee, G. Giri, J. Xu, Do H. Kim, H. A. Becerril, R. M. Stoltenberg, T. H. Lee, Gi Xue, S. C. B. Mannsfeld, Z. Bao, *Nat. Mater.,* 2013, **12**, 665
27 A. Fraleoni-Morgera, L. Benevoli, B. Fraboni, *J. Cryst. Growth* 2010, **312**, 3466
28 C. Reese , Z. Bao, *Mater. Today* 2007 , **10** , 20; J. Lee, S. Roth, Y. Park*, Appl. Phys. Lett*. 2006 **88** 25216.
29 B. Fraboni, C. Femoni, I. Mencarelli, L. Setti, R. Di Pietro, A. Cavallini, A. Fraleoni-Morgera, *Adv. Mater.* 2009, **21**, 1835
30 B. Fraboni, R. DiPietro, A. Castaldini, A. Cavallini, A. Fraleoni-Morgera, L. Setti, I. Mencarelli, C. Femoni, *Org. Electr.* 2008, **9**, 974
31 B. Fraboni, A. Fraleoni-Morgera, A. Cavallini*, Org. Electr*. 2010, **11**, 10
32 D. Braga, N. Battaglini, A. Yassar, G. Horowitz, M. Campione, A. Sassella, A. Borghesi*, Phys. Rev. B* 2008**, 77**, 115205; M. Lampert , P. Mark , "*Current Injection in Solids*" , Academic Press New York 1970
33 J. Trotter*, Acta Cryst*. 1960 **13**, 95
34 E. Capria, L. Benevoli, A. Perucchi, B. Fraboni, M. Tessarolo, S. Lupi, A. Fraleoni-Morgera*, J. Phys. Chem. A* 2013, **117**, 6781
35 A. Fraleoni-Morgera, M. Tessarolo, A. Perucchi, L. Baldassarre, S. Lupi, B. Fraboni, *J. Phys. Chem. C* 2012, **116**, 2563
36 A.Ciavatti, E.capria, A.fraleoni-Morgera, G.Tromaba, D.Dreossi, P.Sellin, B.Fraboni 2014,submitted for publication